THE JOURNAL OF PHYSICAL CHEMISTRY B

Article

pubs.acs.org/JPCB

Decompression-Induced Crystal Polymorphism in a Room-Temperature Ionic Liquid, *N*,*N*-Diethyl-*N*-methyl-*N*-(2-methoxyethyl) Ammonium Tetrafluoroborate

Yukihiro Yoshimura,*[,†] Hiroshi Abe,[‡] Yusuke Imai,[‡] Takahiro Takekiyo,[†] and Nozomu Hamaya[§]

[†]Department of Applied Chemistry, National Defense Academy, Yokosuka, Kanagawa 239-8686, Japan

[‡]Department of Materials Science and Engineering, National Defense Academy, Yokosuka, Kanagawa 239-8686, Japan

[§]Graduate School of Humanities and Sciences, Ochanomizu University, Tokyo 112-8610, Japan

ABSTRACT: We explore the phase behavior of room-temperature ionic liquids (RTILs) compressed under high pressure to determine whether they crystallize or hold a liquid state. RTILs have attractive supercooling properties compared with ordinary molecular liquids, which easily become a glassy state without crystallizing at ambient pressure. Thus, phase behavior under extreme stress, such as pressure, might yield interesting results. Here, we show that *N*,*N*-diethyl-*N*-methyl-*N*-(2-methoxyethyl) ammonium tetrafluoroborate ([DEME][BF_4]) could be crystallized upon compression, but it usually formed a superpressed liquid. Alternatively, unusual crystallization could be induced by releasing the pressure on the superpressed liquid. Notably, crystal polymorphism was observed in the decompression process. These facts along with visual observations indicate the possibility of [DEME][BF_4] serving as a superpressurized glass. Our findings may facilitate the development of a new range of applications for RTILs that have undergone high-pressure recrystallization.

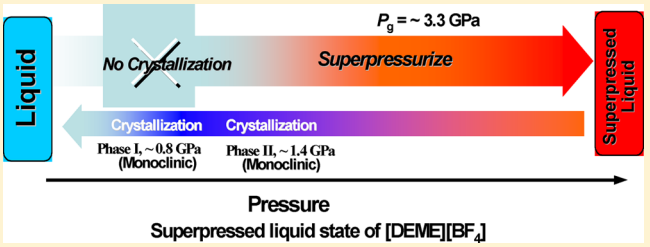

INTRODUCTION

The liquid structure of room-temperature ionic liquids (RTILs) consisting of organic cations and inorganic anions is characterized by a balance between long-range Coulomb electrostatic forces among the constituent ions and local geometric factors.[1,2] These features are key to preventing ions from crystallizing, and most RTILs are easily supercooled and form glasses.

Since interactions strongly depend on intermolecular distances, high pressure is an excellent probe for molecular liquids.[3] Hence, it would be worthwhile to explore the intermolecular potential through both attractive and repulsive sides under varying under high-pressure conditions. As a common knowledge, we expect that liquids eventually crystallize upon compression due to the molecular ordering. However, if we compress an RTIL, which consists of only charged ions using pressure as an external factor, what will happen to the phase behavior? Will crystallization occur or will it hold a liquid state up to very high pressure? It is most likely that competition among various types of interactions determines phase transitions and affects crystallization. In light of these properties and to further extend the applicability of this promising substance, it would be useful to gain a deeper understanding of how pressure affects the phase behavior of an RTIL.

There have been prior reports on related substances under high pressure.[4−15] In previous studies, the room-temperature phase transition behavior of two typical (prototype) imidazolium-based ionic liquids, 1-butyl-3-methylimidazolium tetrafluoroborate ([bmim][BF_4])[11] and 1-butyl-3-methylimidazolium hexafluorophosphate ([bmim][PF_6]),[12] was reported: [bmim][PF_6] easily crystallizes upon compression (~0.1 GPa), whereas [bmim][BF_4] does not crystallize but shows phase transitions up to 30 GPa. The authors[11] postulated that pressure-induced amorphization of [bmim][BF_4] probably occurs at 21.26 GPa, though we feel that the evidence is inconclusive.

Here, we present the first observation of unique behavior on an aliphatic quaternary ammonium-based ionic liquid in which the cation has a flexible methoxyethyl group on the nitrogen atom,[16] *N*,*N*-diethyl-*N*-methyl-*N*-(2-methoxyethyl) ammonium tetrafluoroborate (denoted as [DEME][BF_4]).

EXPERIMENTAL METHODS

As an ionic liquid, we used *N*,*N*-diethyl-*N*-methyl-*N*-(2-methoxyethyl) ammonium tetrafluoroborate, [DEME][BF_4] (Kanto Chemical Co.; Cl < 0.01%, *F* < 0.005%, Na < 0.005%, H_2O < 0.05%). The concentration of water contained in the [DEME][BF_4] as-received sample was doubly checked to be less than 126 ppm on the basis of the Karl Fischer titration method.

Received: January 11, 2013
Revised: February 17, 2013
Published: February 21, 2013

   dx.doi.org/10.1021/jp400341r | *J. Phys. Chem. B* 2013, 117, 3264−3269

High-pressure Raman spectra were obtained with a diamond anvil cell (DAC). In the DAC, few ruby balls and the sample were sealed by a stainless steel gasket 0.35−0.40 mm in diameter and approximately 0.25 mm thick, which had been preindented from an original thickness of 0.26 mm. Diamond anvils were cut from low-fluorescent, type-I diamonds (culet 0.6 mm). Raman spectra were typically measured by a JASCO NR-1800 spectrophotometer. The DAC was mounted under the microscope of a Raman spectrophotometer. The 514.5 nm line of argon-ion laser excitation (~350 mW) was typically used. All the sample preparations were done in a drybox to avoid atmospheric H_2O and CO_2.

High-pressure X-ray diffraction measurements were carried out with the DAC on beamline BL-18C of the Photon Factory at the High Energy Accelerator Research Organization in Japan. A cylindrical focusing mirror was placed in front of a double monochromator of Si(111). The incident X-ray beam was collimated to be 100 μm in diameter. The incident wavelength was estimated to be 0.061872 nm calibrated with a CeO_2 standard. An imaging plate system (BAS2000, Fuji-Film Co., Japan) was selected to obtain two-dimensional Debye rings.[17] To reduce the preferred orientation on the Debye rings, two-dimensional data were reduced into one-dimensional diffraction patterns. The observed X-ray diffraction patterns were analyzed by FOX, which is characterized by ab initio crystal structure determinations.[18]

All the Raman and X-ray diffraction data were collected as the sample was compressed in steps. The pressure was determined from the spectral shift of the R_1 fluorescence line of the ruby ball in the sample chamber of the DAC.[19,20] In recording the data, pressure was increased at intervals from 10 to 20 min.

RESULTS AND DISCUSSION

First, we show pressure-induced Raman spectral changes of [DEME][BF_4] in Figure 1. Raman spectroscopy is often used to explore phase changes and/or bonding structures of liquids, because it provides information on the local structure in the liquid state. The observation of C−H stretching vibration from RTILs can serve as a useful probe to determine structural changes.[4] The wavenumber region from 2800 to 3200 cm^{-1} is the C−H stretching mode (ν_{CH}) from the alkyl chain of the [DEME] cation. Although the detailed peak assignments of the ν_{CH} modes for the [DEME] cation are not currently available, and thus, the spectra present difficulties for quantitative interpretation, four distinct peaks (①−④) are conceivable.

A notable feature of the pressure-induced spectral change is that the peak intensity around 3000 cm^{-1}, designated as ① (Figure 1), increases with increasing pressure, and at ~2.6 GPa, the peak intensities of ① and ② become almost comparable. Upon subsequent compression, the two peaks merge into one asymmetric broad band. Above ~5 GPa, the spectral resolution of each peak becomes unclear. Finally, the spectrum at 5.5 GPa shows a completely different feature from that at 0.1 MPa. A closer look at the results shows that peak ④ becomes unclear with increasing pressure and seems to disappear near 1.5 GPa. We expect that there exists a discontinuity in the frequency shifts. Upon compression, the ν_{CH}, C_4N symmetric, and BF_4^- stretching bands, overall, shift to higher frequencies, but a slight bit of change in the slopes occurs in the shifts of the ν_{CH} around 1 GPa, as shown in Figure 2. The full width at half-maximum (fwhm) of Raman spectra of [DEME][BF_4] under different pressures is shown in Figure 3. A small bump is

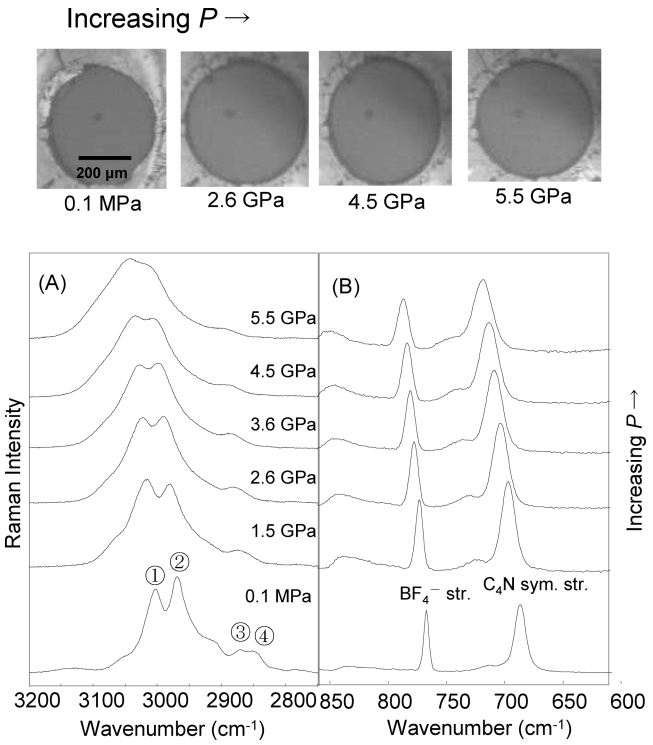

Figure 1. Raman spectral changes in (A) CH stretching and (B) lower-frequency vibrational modes (BF_4^- and C_4N symmetric stretching bands) of [DEME][BF_4] at room temperature as a function of pressure. The $P-T$ conditions were 0.1 MPa ~ 5.5 GPa and 298 K. Upper: Photomicrographs in the sequence of elevated pressures. We note that, apparently, boundaries indicating crystal domains were not observed in the sample texture, and the was sample maintained in the (probably metastable) liquid state across the pressure range from ambient to 5.5 GPa.

conceivable in the C_4N symmetric (higher-frequency) and BF_4^- stretching bands around ~1 GPa. More remarkably, the fwhm's for the CH stretching band are almost flat in the pressure region of 1.5−3.3 GPa, followed by a steep increase again above ~3.3 GPa due to the application of pressure. These features imply that a structural perturbation is occurring around the 1−1.5 GPa region. It is most likely that these spectral features arise from changes in geometrical properties of the bonding network, such as the contraction of C−H bonds and the enhancement of the overlap repulsion effect due to hydrostatic pressure.[5]

A major surprise in this investigation was the noncrystallizing of this material in the range of 5.5 GPa at room temperature, which is consistent with visual inspections in the sequence of elevated pressures, shown in Figure 1 (upper). This state was also analyzed by synchrotron X-ray diffraction measurements. The diffraction profile had a halo pattern typical of a liquid or amorphous material, and it is clear that at least this phase is not a crystalline state. The observations may indicate a pressure-induced structural change in [DEME][BF_4]. We then aimed to confirm the phase of [DEME][BF_4] under a pressure of 5.5 GPa.

To this end, we can gain some insight from the pioneering work on the ruby pressure scale by Piermarini et al.[21] They showed that the broadening of the ruby R_1 line observed in a hydrostatic environment is independent of ruby's particle size and gasket dimensions. However, if nonhydrostatic stress states exist, then line-broadening will occur based on the magnitude of the gradient and the local stress state. It is important to note

dx.doi.org/10.1021/jp400341r | J. Phys. Chem. B 2013, 117, 3264−3269

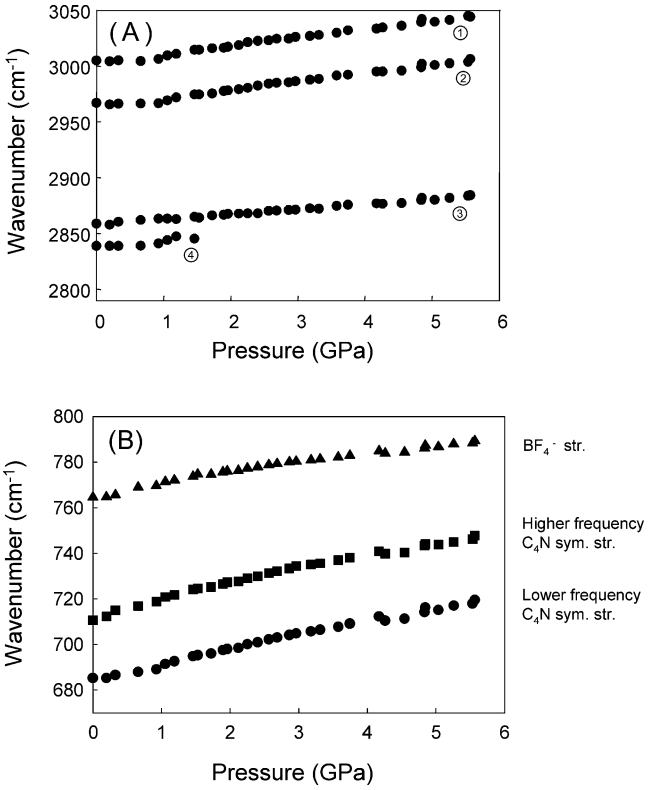

Figure 2. Raman-frequency shifts in the (A) CH stretching and (B) BF_4^- and C_4N symmetric stretching bands of [DEME][BF_4] as a function of pressure. The numbers ①–④ in (A) correspond to the peaks of the [DEME] cation in Figure 1A.

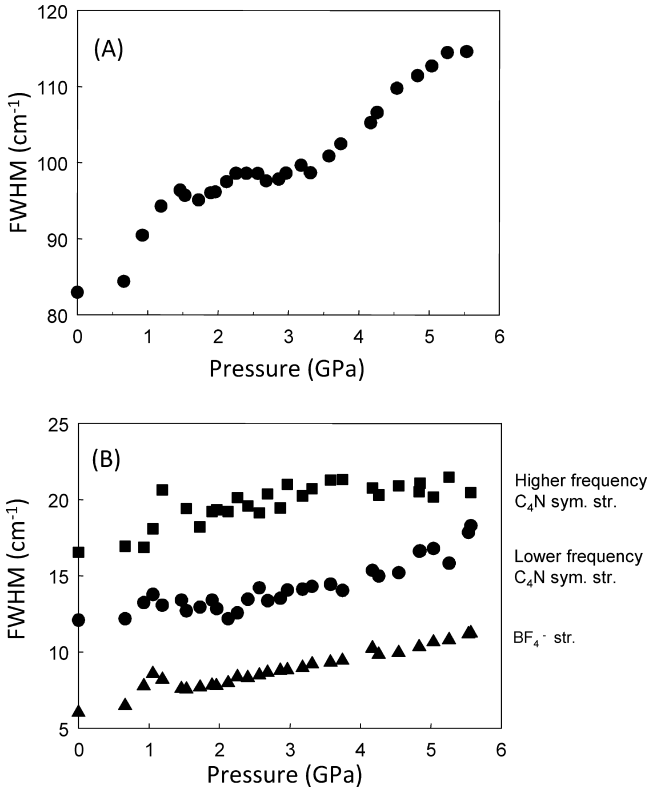

Figure 3. Changes in the full width at half-maximum, fwhm, of Raman (A) CH stretching and (B) lower-frequency vibrational modes (BF_4^- and C_4N symmetric stretching bands) of [DEME][BF_4] as a function of pressure at 298 K.

that this technique for measuring local stresses has potential in fundamental studies on glass formation induced by pressure, particularly with respect to variations in the glass transition points as a function of pressure.[21]

The pressure evolution of the fwhm of R_1 spectra relative to the 0.1 MPa line width is shown in Figure 4. We can see that the onset of line-broadening is rather abrupt and that the broadening rapidly increases with pressure above the initiation point, which is estimated to be around 3.3 GPa. According to the previous study,[21] the initiation point is interpreted as an approximate measurement of the glass transition (vitrification) pressure. Therefore, we interpret that [DEME][BF_4] can be superpressed (overpressurized) into a metastable state without crystallizing. On the basis of the spectral features in Figures 1–4 mentioned above, we think that the structural perturbation toward the vitrification was locally starting around 1∼1.5 GPa and completed over 3.3 GPa.

It is, however, important to mention that, in our study, we observed that the sample occasionally crystallized at a 0.7–1.0 GPa range upon being pressurized, in which case pressure-induced vitrification is not measurable. We hypothesize that, because different states might exist at comparable thermodynamic conditions, several local conformational minima in the potential energy surface could occur.[22] If the application of pressure on [DEME][BF_4] increases the disorder in its structure and if such disorder is frozen in at high pressures, glass forms. This might be one of the reasons for the easy superpressurizing of [DEME][BF_4] with the bypassing of solidification. Compression rate, sample volume in the DAC, and subsequent cooperatively dynamics leading to the formation of the reaction seeds for the phases may play a

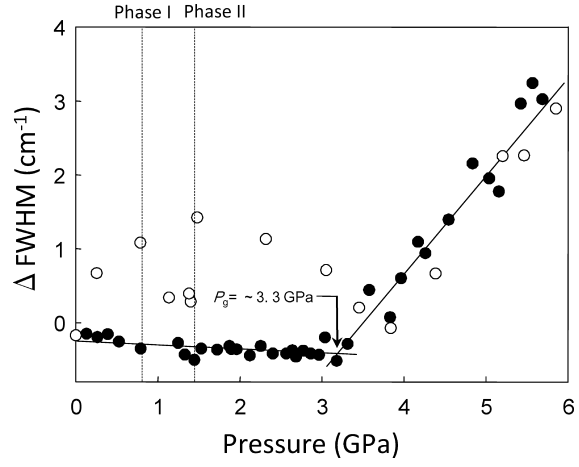

Figure 4. Pressure broadening of the sharp ruby R_1 fluorescence line (full width at half-maximum, fwhm) relative to the 0.1 MPa line width (●, compression; ○, decompression). The solid and dashed lines are guides to the eyes. P_g corresponds to the vitrification pressure. We can find this kind of superpressurizing in the case of some liquids such as methanol.[21,23] If compressed sufficiently rapidly beyond the crystallization pressure, methanol slowly vitrifies rather than crystallizes.

fundamental role, though we could not find the definitive factor(s) in controlling the responses; that is, sometimes we could get crystal and other times get glass. More extensive investigations are mandatory to solve this point.

On the other hand, glassy states generally show a hysteresis depending on external fields, such as temperature and pressure.

dx.doi.org/10.1021/jp400341r | J. Phys. Chem. B 2013, 117, 3264–3269

Thus, the behavior of fwhm of ruby R_1 spectra in the decreasing process of pressure is interesting. The value decreases with decreasing pressure down to ca. 4 GPa, but, interestingly, below 4 GPa, the Δfwhm shows zigzag behavior at small maxima of around 1.5 and 0.8 GPa (Figure 4). These results may be explained by that a relaxation of the sample occurred in the glassy solid with respect to the decreasing pressure process, which will be discussed below.

Such a metastable phase remained stable at room temperature up to the highest pressure that we reached, that is, ∼5.5 GPa. However, remarkably, upon a pressure decrease down to ca. 1.4 GPa (Figure 5), this phase underwent a phase transition,

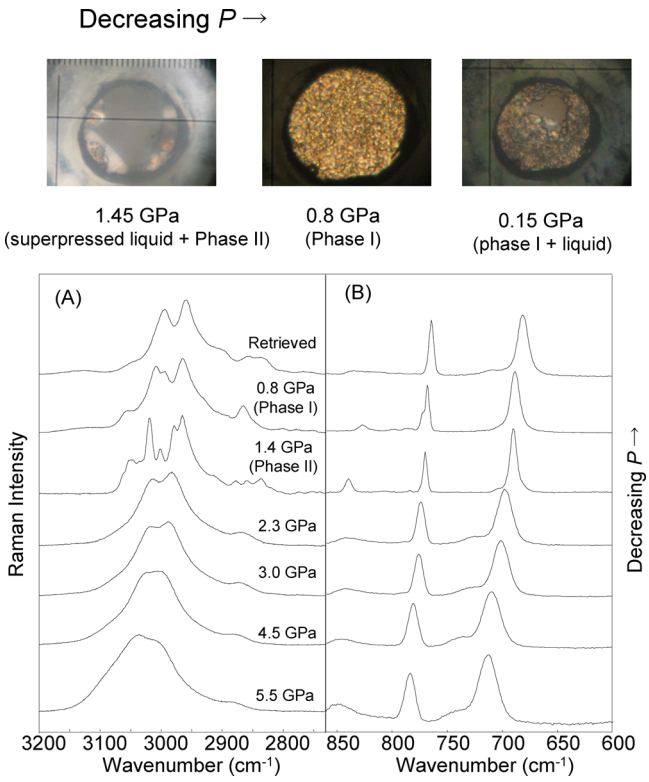

Figure 5. Raman spectral changes showing decompression-induced crystal polymorphism in [DEME][BF_4] at 298 K. (A) CH stretching and (B) lower-frequency vibrational modes (BF_4^- and C_4N symmetric stretching bands) of [DEME][BF_4]. Upper: The sample changed gradually from a transparent superpressed liquid state into, first, the crystalline solid phase II growing up from the edge of a gasket at 1.45 GPa, then to phase I (fine grains) at 0.8 GPa, and, finally, to the normal liquid state melting from the upper center region around 0.15 GPa with releasing pressure.

leading to a crystalline phase (hereafter, phase II) exhibiting a completely different Raman spectrum from that of the HP-crystal. (The spectra of a sample in which crystallization occurred on compression are designated as HP-crystal.) We can find such a statement in the 1980 paper by Mammone et al.[23] that crystallization of methanol could sometimes be induced by releasing pressure on the glass. Even more remarkable was the fact that, upon a further decrease in pressure from phase II, we observed another phase transition to a crystalline phase (phase I) at 0.8 GPa. In situ photomicrographic observations of [DEME][BF_4] with decreasing pressure are also shown in Figure 5 (upper). The phenomenon of decompression-induced crystallization may resemble a "cold crystallization", which is observable in the relaxation from the glassy sample upon heating at ambient pressure.[24] It is also interesting to refer to the former results of *N*,*N*-diethyl-*N*-methyl-*N*-(2-methoxyethyl) ammonium bis(trifluoromethylsulfonyl)imide, [DEME][TFSI], which has a different anion from [DEME][BF_4]. [DEME][TFSI] shows complete reversibility of the pressure effects if the pressure is released from 5.5 GPa down to 0.1 MPa, and decompression-induced crystallization does not occur.[25]

These observations suggest very similar energies for the phases making the changes kinetically driven. Actually, in one experiment, we have followed a retention-time effect on the sample at ∼1 and ∼4 GPa for 6 months without observing any spectral changes, suggesting the attainment of the stable phases. However, in another experiment, the sample was held at ∼1 GPa only for 15 h, giving rise to a phase change to HP-crystal, despite that the duration of the time was, in this case, much shorter than that performed former case. This phase behavior keeping at high pressures remarks the key role of kinetics in determining the metastabilities. Additionally, decompression of the glassy sample normally brought the formation of phase II at 1.4 GPa. However, upon more quick decompression through this pressure range (>0.5 GPa/h), once we have experienced that the glass transformed to phase I at ∼1 GPa, which also shows to be caused by a kinetically driven phenomenon.

In the past, decompression-induced crystallizations of molecular liquids and hydrated silica-rich melts (as a model compound for magma) have been reported.[28−30] For example, Fanetti, et al.[28] described the observation of the kinetically hindered phase II of pyridine upon decompression. On the other hand, for interpreting natural magma ascent processes in a volcano dominating the style of volcanic activity, the complicated mechanisms on decompression-induced crystallization were explained by a cooling effect (magma cooling) and a dehydration effect (magma decompression) along with the kinetic effect.[29] Decompression induces the crystallization, because a decrease in the water solubility (degassing) causes volatile exsolution, and a subsequent increase in the temperature at which mineral phases form. Nucleation and growth rates highly depend on the effective undercooling (difference between the crystal liquidus temperature and the magma temperature).

The results of representative X-ray diffraction patterns for phases I and II are displayed in Figure 6. Analyzed crystallographic data are summarized in Table 1. Both high-pressure crystals were uniquely determined to be monoclinic lattices ($Z = 4$ for phase II and $Z = 2$ for phase I, where Z is the number of molecules per unit cell). It is interesting to point out that the crystal structure of pure [DEME][BF_4] at ambient pressure and low temperature was proposed to be a mixture of monoclinic and orthorhombic.[26,27] The crystallization temperature T_c was around 243 K, as determined by in situ simultaneous X-ray and DSC measurements. Importantly, the crystal structures of high-pressure phases are different from that of the low-temperature phase at ambient pressure.

For a complementary insight into the responses to pressure and temperature changes, it is interesting to compare the Raman spectra of a low-temperature induced crystal at 0.1 MPa, crystal phase II, HP-crystal, crystal phase I, liquid state at 0.1 MPa, glassy state at 0.1 MPa and 77 K, and superpressed (glassy) state at 5.5 GPa and 298 K (Figure 7). It is to be noted that [DEME][BF_4] easily forms a glassy state at low temperatures upon quick cooling at 0.1 MPa.[31] In a separate measurement, we observed that [DEME][BF_4] has a glass

dx.doi.org/10.1021/jp400341r | J. Phys. Chem. B 2013, 117, 3264−3269

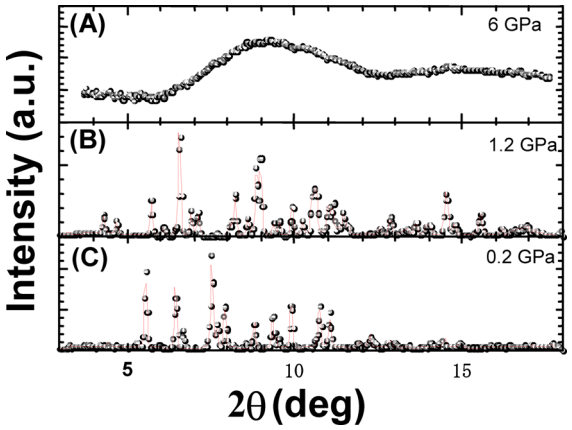

Figure 6. X-ray diffraction patterns showing the decompression-induced crystal polymorphism in [DEME][BF_4] at 298 K. (A) Superpressed state at ∼6 GPa, (B) phase II at ∼1.2 GPa, and (C) phase I at ∼0.2 GPa. The calculated results are represented by red curves. The calculated peak positions are in good agreement with the observed ones, though the peak intensities have minor discrepancies due to the preferred orientations on the Debye rings.

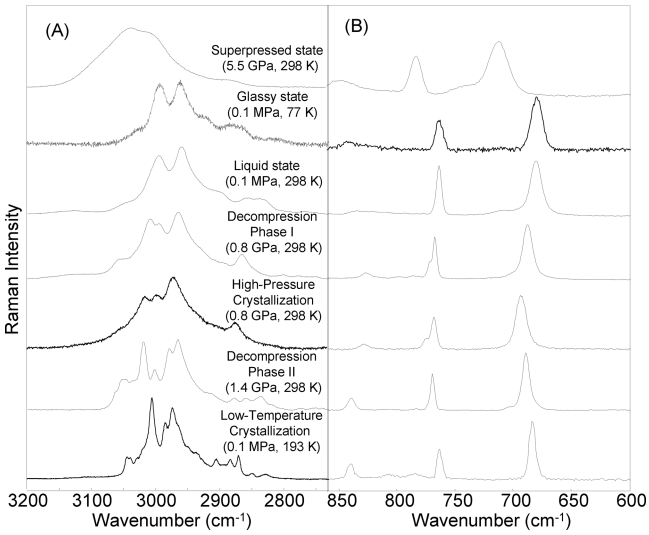

Figure 7. Comparison of the Raman spectra of [DEME][BF_4] at various $P-T$s. (A) The CH stretching vibrational region and (B) the lower-frequency vibrational region (BF_4^- and C_4N symmetric stretching bands). Temperature-induced Raman spectral changes at ambient pressure were controlled with a LINKAM THMS-600 (Japan Hightech Co.). In view of the results, the Raman spectrum of the solid crystallized by applied pressure (HP-crystal at 0.8 GPa, 298 K) is totally different from that at low temperature (0.1 MPa, 193 K). When the samples crystallized upon compression, a peak around 3000 cm^{-1} splits and a broad band around 2850 cm^{-1} becomes sharp.

transition temperature of 173 K. We find that the glassy spectrum at 0.1 MPa and 77 K basically shows a feature similar to that of the liquid state at 298 K and 0.1 MPa. Although an essentially quantitative explanation of the actual structural differences between the low-temperature and the high-pressure glasses is difficult at present, the spectrum of the superpressed state may look to be similar to a pressure broadened version of the glassy state at 0.1 MPa and 77 K. We can see a gradual shift of the band centers apart from the small change in the slopes around 1 GPa in Figure 2A, accounting for a smooth evolution of the corresponding Raman bands. Accordingly, the straightforward interpretation of these results would be that the structures are just changing because of the pressure. Of course, there may be another possibility that the superpressed state at 5.5 GPa and 298 K is structurally different from the glassy state at 0.1 MPa and 77 K. In this case, there may be a variety of metastable states available to the amorphous solid, which is accessed by different pressure−temperature paths. The extent, however, remains an open question for further experimental study. It is interesting to point out that, among the pressure-induced crystals, similarities in spectral shapes and characterizations were recognized (but not identical) between phase I and HP-crystal, and between phase II and the low-temperature crystal at 0.1 MPa. It is difficult to say more about whether the HP-crystal is structurally the same state as the phase I, as, unfortunately, we could not get the X-ray data of the HP-crystal in a timely manner in the present study. Anyway, these results demonstrate that there is large variability in the phase behavior of [DEME][BF_4] with respect to external factors.

In summary, we have demonstrated that [DEME][BF_4] can be overpressurized and enters a superpressed liquid at ∼3.3 GPa. As the present results show, pressure plays a critical role in regulating the structure and properties of materials. Subjecting materials to high pressure is a unique tool for new explorations in material chemistry as it enables us to create novel substances and alter the properties of existing compounds. Pressure may also be used as a means to explore as yet unexplained properties of fluids and solids. We believe that the present study provides useful insights into the phase behavior of RTILs under several conditions. A detailed understanding of the phase behavior/diagram of RTILs is of great importance for further extending the range of applications for these important materials. RTILs are expected to play a crucial role in environmentally friendly applications when used as solvents, because they are difficult to evaporate, which prevents the pollution of the environment. However, precisely because of this property, distillation through evaporation, which is important for recycling and purifying common organic solvents, cannot be applied to RTILs.[7,10] Thus, one direct

Table 1. Crystal Data of the Low-Temperature and High-Pressure Phases[a]

crystal		a (nm)	b (nm)	c (nm)	β (deg)	Z	ρ (g/cm^3)	wR (%)	R (%)
low-temperature phase	monoclinic	1.632	1.009	0.896	123.8	4	1.26	19.5	15.6
	orthorhombic	1.012	1.347	0.893	90.0	4			
phase II (1.2 GPa)	monoclinic	0.791	1.081	1.342	107.9	4	1.42	22.3	18.6
phase I (0.2 GPa)	monoclinic	1.032	0.521	1.147	107.6	2	1.32	27.9	23.9

[a]The weighted reliability and conventional factors are expressed as wR and R, respectively. Z is the number of molecules per unit cell. Considering the liquid density at room temperature and ambient pressure (ρ = 1.17 g/cm^3), crystal structures at high pressures seem to be well-optimized despite the large blind angles in the DAC.

dx.doi.org/10.1021/jp400341r | J. Phys. Chem. B 2013, 117, 3264−3269

application of the present findings might be the high-pressure recycling or purification of RTILs[9] since pressure-induced crystallization of RTILs is thus far known to be a rare phenomenon.[4−15] The present results are expected to constitute an initial, but significant step, in such an investigation.

AUTHOR INFORMATION

Corresponding Author

*E-mail: muki@nda.ac.jp.

Notes

The authors declare no competing financial interest.

ACKNOWLEDGMENTS

We would like to acknowledge Prof. M. Kato and Mr. R. Wada of Ritsumeikan University for experimental support.

REFERENCES

(1) Welton, T. Room-Temperature Ionic Liquids. Solvents for Synthesis and Catalysis. *Chem. Rev.* **1999**, *99*, 2071−2084.

(2) Earle, M. J.; Seddon, R. Ionic Liquids. Green Solvents for the Future. *Pure Appl. Chem.* **2000**, *72*, 1391−1398.

(3) Polian, A.; Loubeyre, P.; Boccara, N. *Simple Molecular Systems at High Pressure*; Plenum: New York, 1988.

(4) Chang, H.-C.; Jiang, J.-C.; Su, J.-C.; Chang, C.-Y.; Lin, S. H. Evidence of Rotational Isomerism in 1-Butyl-3-methylimidazolium Halides: A Combined High-Pressure Infrared and Raman Spectroscopic Study. *J. Phys. Chem. A* **2007**, *111*, 9201−9206.

(5) Chang, H. C.; Jiang, J. C.; Chang, C. Y.; Su, J. C.; Hung, Y. C.; Liou, Y. C.; Lin, S. H. Structural Organization in Aqueous Solutions of 1-Butyl-3-methylimidazolium Halides: A High-Pressure Infrared Spectroscopic Study on Ionic Liquids. *J. Phys. Chem. B* **2008**, *112*, 4351−4356.

(6) Umebayashi, Y.; Jiang, J.-C.; Shan, Y.-L.; Lin, K.-H.; Fujii, K.; Seki, S.; Ishiguro, S.; Lin, S. H.; Chang, H.-C. Structural Change of Ionic Association in Ionic Liquid/Water Mixtures: A High-Pressure Infrared Spectroscopic Study. *J. Chem. Phys.* **2009**, *130*, 124503.

(7) Chang, H.-C.; Jiang, J.-C.; Liou, Y.-C.; Hung, C.-H.; Lai, T.-Y.; Lin, S. H. Effects of Water and Methanol on the Molecular Organization of 1-Butyl-3-methylimidazolium Tetrafluoroborate As Functions of Pressure and Concentration. *J. Chem. Phys.* **2008**, *129*, 044506.

(8) Chang, H.-C.; Jiang, J.-C.; Liou, Y.-C.; Hung, C.-H.; Lai, T.-Y.; Lin, S. H. Local Structure of Water in 1-Butyl-3-methylimidazolium Tetrafluoroborate Probed by High-Pressure Infrared Spectroscopy. *Anal. Sci.* **2008**, *24*, 1305−1309.

(9) Su, L.; Li, L.; Hu, Y.; Yuan, C.; Shao, C.; Hong, S. Phase Transition of $[C_n\text{-mim}][PF_6]$ under High Pressure up to 1.0 GPa. *J. Chem. Phys.* **2009**, *130*, 184503.

(10) Su, L.; Li, M.; Zhu, X.; Wang, Z.; Chen, Z.; Li, F.; Zhou, Q.; Hong, S. In Situ Crystallization of Low-Melting Ionic Liquid $[BMIM][PF_6]$ under High Pressure up to 2 GPa. *J. Phys. Chem. B* **2010**, *114*, 5061−5065.

(11) Su, L.; Zhu, X.; Wang, Z.; Cheng, X.; Wang, Y.; Yuan, C.; Chen, Z.; Ma, C.; Li, F.; Zhou, Q.; Cui, Q. In Situ Observation of Multiple Phase Transitions in Low-Melting Ionic Liquid $[BMIM][BF_4]$ under High Pressure up to 30 GPa. *J. Phys. Chem. B* **2012**, *116*, 2216−2222.

(12) Russina, O.; Fazio, B.; Schmidtc, C.; Triolo, A. Structural Organization and Phase Behaviour of 1-Butyl-3-methylimidazolium Hexafluorophosphate: An High Pressure Raman Spectroscopy Study. *Phys. Chem. Chem. Phys.* **2011**, *13*, 12067−12074.

(13) Imai, Y.; Takekiyo, T.; Abe, H.; Yoshimura, Y. Pressure- and Temperature-induced Raman Spectral Changes of 1-Butyl-3-methylimidazolium Tetrafluoroborate. *High Press. Res.* **2010**, *31*, 53−57.

(14) Takekiyo, T.; Imai, Y.; Hatano, N.; Abe, H.; Yoshimura, Y. Pressure-induced Phase Transition of 1-Butyl-3-methylimidazolium Hexafluorophosphate $[bmim][PF_6]$. *High Press. Res.* **2010**, *31*, 35−38.

(15) Yoshimura, Y.; Takekiyo, T.; Imai, Y.; Abe, H. High Pressure Phase Behavior of Two Imidazolium-Based Ionic Liquids, $[bmim][BF_4]$ and $[bmim][PF_6]$. In *Ionic Liquids: Classes and Properties*; Handy, S. T., Ed.; InTech Publishing: Rijeka, Croatia, 2011; Chapter 8, pp 187−202.

(16) Sato, T.; Masuda, G.; Takagi, K. Electrochemical Properties of Novel Ionic Liquids for Electric Double Layer Capacitor Applications. *Electrochim. Acta* **2004**, *49*, 3603−3611.

(17) Shimomura, O.; Takemura, K.; Fujihisa, H.; Fujii, Y.; Ohishi, Y.; Kikegawa, T.; Amemiya, Y.; Matsushita, T. Application of an Imaging Plate to High-Pressure X-ray Study with a Diamond Anvil Cell. *Rev. Sci. Instrum.* **1992**, *63*, 967.

(18) Favre-Nicolin, V.; Černý, R. FOX, 'Free Objects for Crystallography': A Modular Approach to *ab Initio* Structure Determination from Powder Diffraction. *J. Appl. Crystallogr.* **2002**, *35*, 734−743.

(19) Mao, H. K.; Bell, P. M.; Shaner, J. W.; Steinberg, D. Specific Volume Measurements of Cu, Mo, Pd, and Ag and Calibration of the Ruby R_1 Fluorescence Pressure Gauge From 0.06 to 1 Mbar. *J. Appl. Phys.* **1978**, *49*, 03276.

(20) Mao, H. K.; Xu, J.; Bell, P. M. Calibration of the Ruby Pressure Gauge to 800 kbar under Quasi-Hydrostatic Conditions. *J. Geophys. Res.* **1986**, *91*, 4673−4676.

(21) Piermarini, G. J.; Block, S.; Barnett, J. D. Hydrostatic Limits in Liquids and Solids to 100 kbar. *J. Appl. Phys.* **1973**, *44*, 5377−5382.

(22) Brazhkin, V. V. Metastable Phases and 'Metastable' Phase Diagrams. *J. Phys.: Condens. Matter* **2006**, *18*, 9643−9650.

(23) Mammone, J. F.; Sharma, S. K.; Nicol, M. Raman Spectra of Methanol and Ethanol at Pressures up to 100 kbar. *J. Phys. Chem.* **1980**, *84*, 3130−3134.

(24) Jeong, Y. G.; Jo, W. H.; Lee, S. C. Synthesis, Structure, and Thermal Property of Poly(trimethylene tetrephthalate-*co*-trimethylene 2,6-naphthalete) Copolymers. *Fibers Polym.* **2004**, *5*, 245−251.

(25) Yoshimura, Y.; Takekiyo, T.; Imai, Y.; Abe, H. Pressure-induced Spectral Changes of Room-Temperature Ionic Liquid, *N*,*N*-Diethyl-*N*-methyl-*N*-(2-methoxyethyl) Ammonium Bis(trifluoromethylsulfonyl)-imide, [DEME][TFSI]. *J. Phys. Chem. C* **2012**, *116*, 2097−2101.

(26) Imai, Y.; Abe, H.; Goto, T.; Yoshimura, Y.; Michishita, Y.; Matsumoto, H. Structure and Thermal Property of *N*, *N*-Diethyl-*N*-methyl-*N*-2-methoxyethyl Ammonium Tetrafluoroborate-H_2O Mixtures. *Chem. Phys.* **2008**, *352*, 224−230.

(27) Imai, Y.; Abe, H.; Yoshimura, Y. X-ray Diffraction Study of Ionic Liquid Based Mixtures. *J. Phys. Chem. B* **2009**, *113*, 2013−2018.

(28) Fanetti, S.; Citroni, M.; Bini, R. Structure and Reactivity of Pyridine Crystal under Pressure. *J. Chem. Phys.* **2011**, *134*, 204504.

(29) Mollard, E.; Martel, C.; Bourdier, J.-L. Decompression-induced Crystallization in Hydrated Silica-rich Melts: Empirical Models of Experimental Plagioclase Nucleation and Growth Kinetics. *J. Petrology* **2012**, *53*, 1743−1766.

(30) Fabbiani, F. P. A.; Levendis, D. C.; Buth, G.; Kuhs, W. F.; Shankland, N.; Sowa, H. Searching for Novel Crystal Forms by *In Situ* High-pressure Crystallisation: The Example of Gabapentin Heptahydrate. *CrystEngComm* **2010**, *12*, 2354−2360.

(31) Imai, Y.; Abe, H.; Miyashita, T.; Goto, T.; Matsumoto, H.; Yoshimura, Y. Two Glass Transitions in *N*,*N*-Diethyl-*N*-methyl-*N*-(2-methoxyethyl) Ammonium Tetrafluoroborate-H_2O Mixed Solutions. *Chem. Phys. Lett.* **2010**, *486*, 37−39.